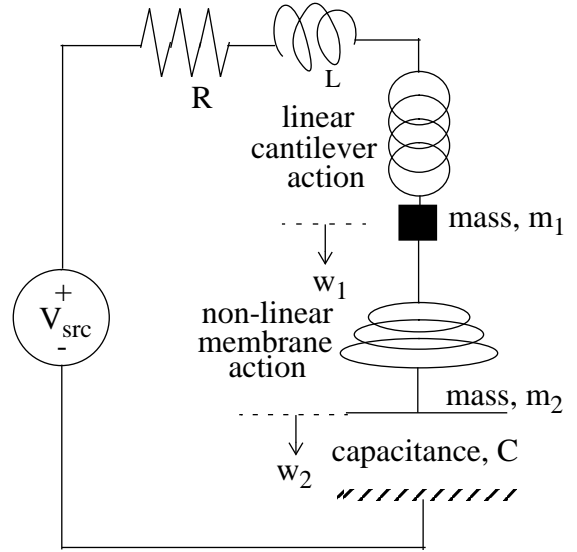
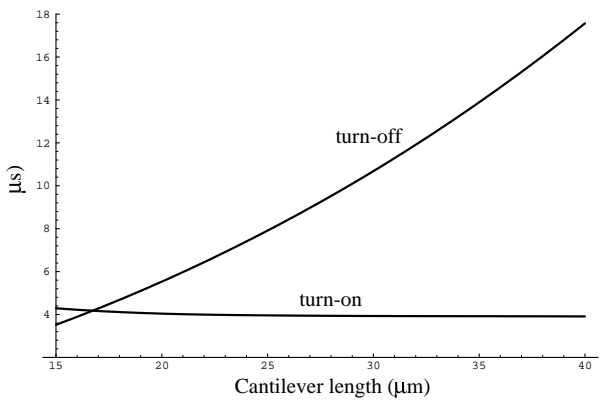
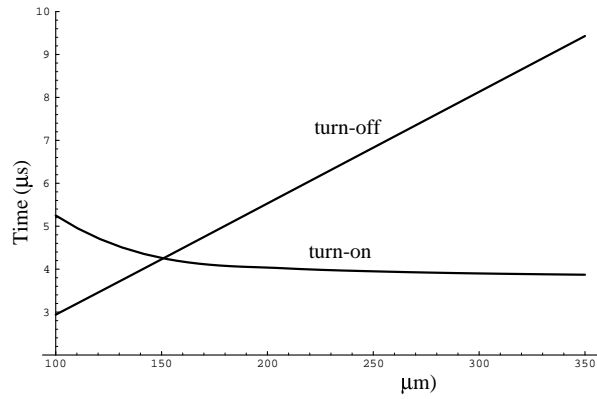


**Fig.11: Current during turn-on**



**Fig.12: Two-lump switch model**



**Fig.8: Turn-on and turn-off times as functions of cantilever length**

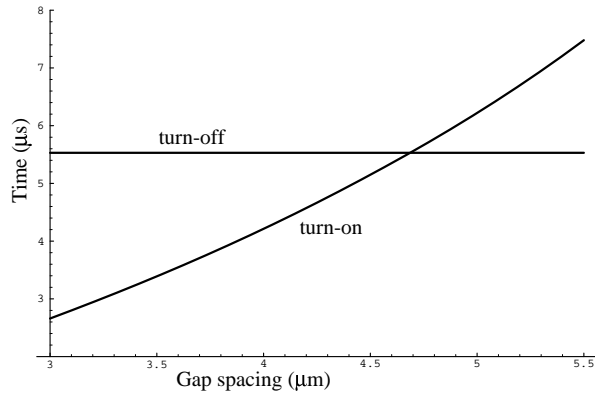


**Fig.9: Turn-on and turn-off times as functions of initial gap spacing**

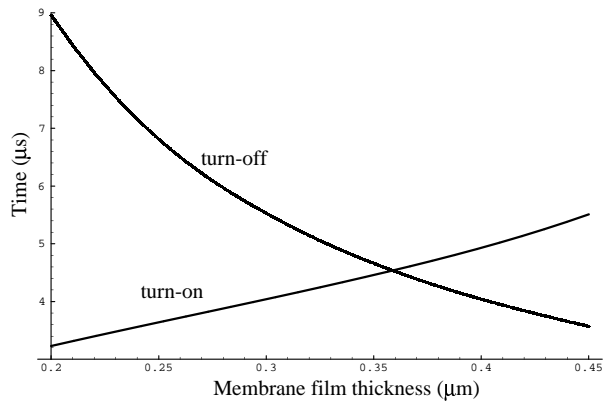


**Fig.10: Turn-on and turn-off times as functions of membrane film thickness**

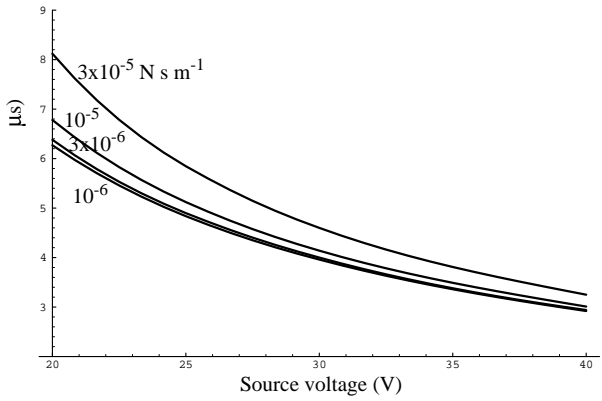
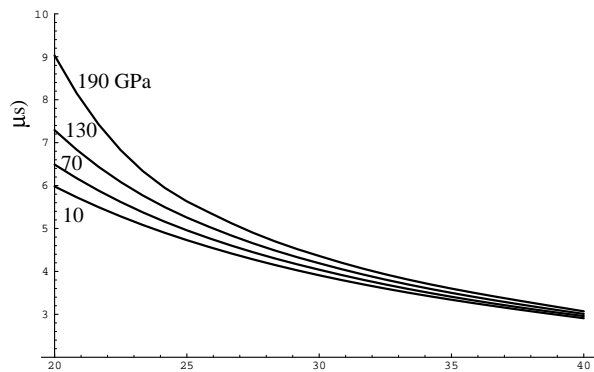


**Fig. 6: Turn-on time vs source voltage for various  $\eta$**

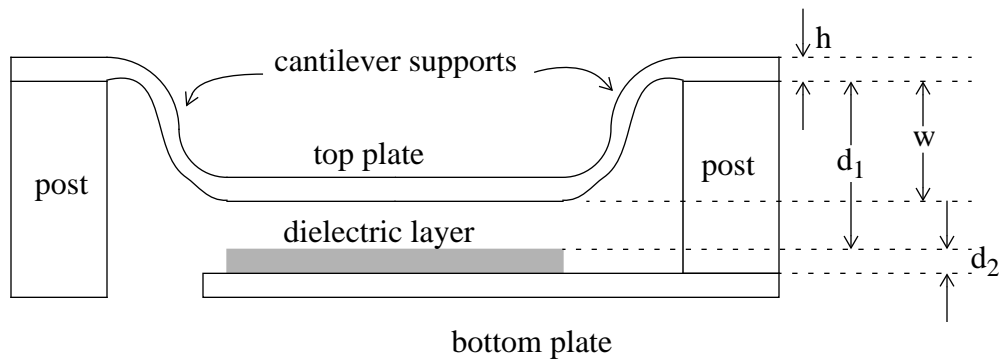


**Fig. 1: Cross-section of micromachined switch**

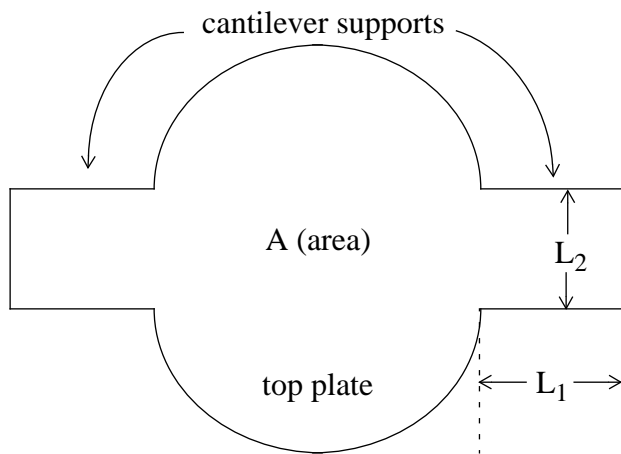


**Fig. 2: Plan view of micromachined switch**

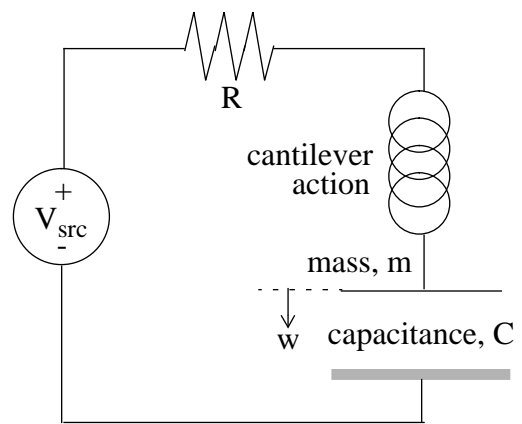


**Fig. 3: One-lump schematic of switch in actuating circuit**

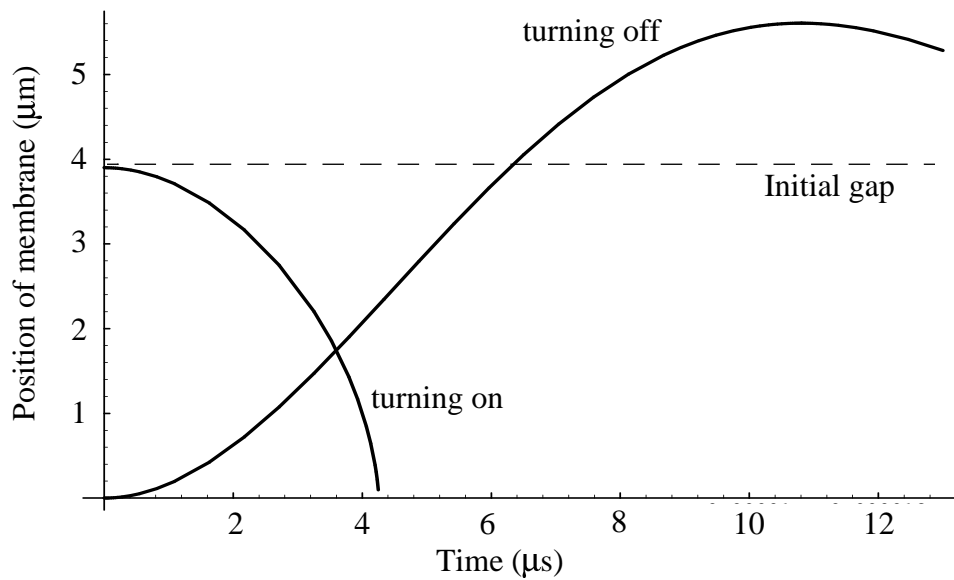


**Fig. 4: Position of membrane as a function of time**

Poisson's ratio.

To include the effect of inductance in the actuating circuit, Eq. (3) can be modified to be

$$V_{src} = V_c + R \left[ \left( \frac{\epsilon A}{d_1 + \frac{d_2}{\kappa} - w_2} \right) \frac{dV_c}{dt} + V_c \left( \frac{\epsilon A}{\left( d_1 + \frac{d_2}{\kappa} - w_2 \right)^2} \right) \frac{dw_2}{dt} \right] + \quad (6)$$

$$L \left\{ \frac{2\epsilon A}{\left( d_1 + \frac{d_2}{\kappa} - w_2 \right)^2} \frac{dw_2}{dt} \frac{dV_c}{dt} + V_c \left[ \frac{2\epsilon A}{\left( d_1 + \frac{d_2}{\kappa} - w_2 \right)^2} \left( \frac{dw_2}{dt} \right)^2 + \left( \frac{\epsilon A}{d_1 + \frac{d_2}{\kappa} - w_2} \right) \frac{d^2 w_2}{dt^2} \right] + \left( \frac{\epsilon A}{d_1 + \frac{d_2}{\kappa} - w_2} \right) \frac{d^2 V_c}{dt^2} \right\}$$

This two-lump model has captured most of the relevant effects of the electrostatically-actuated micromachined switch. The additional parameter  $\sigma$  allows one more degree of freedom in fitting the simulated curves to measurements. Also, through a mixed-mode circuit simulator [8], the lumped model can be embedded into SPICE for full transient and harmonic studies. Finite-element simulations and more measurements are necessary to characterize stiction and initial deformation of the switch.

## REFERENCES

- [1] C. Goldsmith, J. Randall, S. Eshelman, T.H. Lin, "Characteristics of micromachined switches at microwave frequencies," in 1996 MTT-S Technical Digest, p1141-1144
- [2] Nathanson, Newell, Wickstrom, Davis, "The resonant gate transistor," IEEE Transactions on Electron Devices, Vol ED-14, No. 3, pp-117-133, 1967
- [3] B.E. Artz, L.W. Cathey, "A finite element method for determining structural displacements resulting from electrostatic forces," Proc IEEE Solid State Sensor and Actuator Workshop, 1992, pp 190-193
- [4] K.E. Petersen, "Dynamic micromechanics on silicon: Techniques and devices," IEEE Trans. of Electron Devices, ED-25, 1978, pp 1241
- [5] D. Maier-Schneider, J. Maibach, "A new analytical solution for the load-deflection of square membranes," JMEMS, Vol 4 no 4, Dec 1995 pp 238-241
- [6] S.P. Timoshenko, J.M. Gere, "Mechanics of materials," D. Van Nostrand Co, 1972
- [7] M.D. Giovanni, "Flat and corrugated diaphragm design handbook," Marcel Dekker, 1982
- [8] S. Beebe, F. Rotella, Z. Sahul, D. Yergeau, G. McKenna, L. So, Z. Yu, K.C. Wu, E.C. Kan, J. McVittie, R.W. Dutton, "Next generation Stanford TCAD -- PISCES 2ET and SUPREM OO7," IEDM Tech. Dig., 1994, p. 213.

The electrical current  $I_e$  in Fig. 3 is given by

$$I_e = C \frac{dV_c}{dt} + V_c \frac{dC}{dt} \quad (2)$$

which is expanded to the parenthesized term in Eq. 3 below:

$$+ \left[ \left( \frac{\epsilon A}{d_1 + \frac{d_2}{\kappa} - w} \right) \frac{dV_c}{dt} + V_c \left( \frac{\epsilon A}{\left( d_1 + \frac{d_2}{\kappa} - w \right)^2} \right) \frac{dw}{dt} \right] = V_{src}. \quad (3)$$

Notice that the current is a non-linear function of the displacement and velocity of the membrane. Figure 4 shows the solution  $w(t)$  of the coupled ordinary differential equations (1) and (3) which compares reasonably well with experimental measurements [1].

The two material parameters required by the model are the modulus of elasticity,  $E$ , and the viscoelasticity coefficient,  $\eta$ . Values of  $E$  for certain thin films can be measured but  $\eta$  is very difficult to determine. Since it is relatively easy to control  $R$  and  $V_{src}$ , parameter extraction can be accomplished by a least-squares fitting of the simulated transient characteristics to measurements with varying  $R$  and  $V_{src}$ . Figures 5 and 6 show  $t_{on}$  as functions of  $V_{src}$  for different values of  $E$  and  $\eta$  respectively. Similar behaviour of  $t_{on}$  with respect to  $R$  are observed.

After the material parameters have been determined, the model can be used to perform scaling studies of the geometry for performance optimization. Figures 7 through 10 show how  $t_{on}$  and  $t_{off}$  change as functions of geometrical parameters such as membrane area, cantilever length, initial gap and film thickness. The tradeoffs between turn-on and turn-off times is evident. Interestingly, the membrane area and cantilever length, once past certain thresholds, have little effect on the turn-on times. The dynamic power dissipation can be computed from  $I_e(t)$  shown in Fig. 11.

### III. AUGMENTED TWO-LUMP MODEL

The one-lump model can be augmented to include the effects of the membrane, gravity and inductance as shown in Fig. 12. One lump describes the motion of the cantilever supports whereas the other lump describes the membrane. The two equations of motion are

$$\left( \frac{\times EI}{L_1^3} \right) w_1 - \eta_1 \frac{dw_1}{dt} + m_1 g + \frac{c_1 h \sigma}{A} (w_2 - w_1) + \frac{c_2 h E}{A^2} (w_2 - w_1)^3 = m_1 \frac{d^2 w_1}{dt^2} \quad (4)$$

$$\frac{\epsilon A}{\left( d_1 + \frac{d_2}{\kappa} - w_2 \right)^2} V_c^2 - \eta_2 \frac{dw_2}{dt} + m_2 g - \frac{c_1 h \sigma}{A} (w_2 - w_1) - \frac{c_2 h E}{A^2} (w_2 - w_1)^3 = m_2 \frac{d^2 w_2}{dt^2} \quad (5)$$

The additional terms to Eq. (1) are the gravitational forces,  $m_i g$ , and the last two terms on the left-hand sides of both Eqs. (4) and (5) which describe the coupling between the membrane and the cantilevers. The force on the membrane as a function of deformation can be modeled by a tensile term (cubic in  $w$ ) and a bending term (linear in  $w$ ) which can include the effect of residual stress  $\sigma$  [7]. The parameters  $c_1$  and  $c_2$  depend on the geometry of the membrane and

# NONLINEAR DYNAMIC MODELING OF MICROMACHINED MICROWAVE SWITCHES

E.K. Chan, E.C. Kan, P.M. Pinsky and R.W. Dutton

*Center for Integrated Systems, CISX 305, Stanford University, Stanford, CA 94305*

## ABSTRACT

**Nonlinear dynamic lumped models of micromachined switches for microwave applications have been formulated and successfully applied to analyses of transient characteristics and geometrical scaling. Parameter extraction through electrical measurements is summarized.**

## I. INTRODUCTION

The micromachined switch [1] has great potential for microwave applications due to its extremely low intermodulation distortion and IC backend technology compatibility. In the past, the switch has been modeled as a parallel plate capacitor and a linear spring at static equilibrium [2]. 3D finite element simulations have been used to examine more detailed geometrical effects [3], but are computationally expensive and mostly limited to static analysis. In this paper, we have formulated a nonlinear dynamic lumped model which models the support cantilevers and membrane separately and includes the effects of inertia, viscoelasticity, the external actuating circuit and residual stress. Parameter extraction for the lumped model from electrical measurements is described. Scaling properties for the geometrical design of the switch are analyzed.

## II. NON-LINEAR DYNAMIC ONE-LUMP MODEL

The modern design and performance optimization of micromachined switches deviates significantly from the simple geometry of cantilevers [4]. The electrostatic force on the top membrane is so inhomogeneous that the approximation of a thin membrane anchored at the periphery under constant pressure is not accurate[5]. It is more accurate and scalable to formulate the lumped model as a rigid diaphragm suspended above a ground plate by two cantilevers. Figures 1 and 2 show the various geometrical parameters in the lumped model. The schematic of the actuating circuit is shown in Fig. 3. To account for the inelastic behavior of the cantilevers, the dynamic equation is given by

$$\frac{1}{2} \frac{\epsilon A}{\left(d_1 + \frac{d_2}{\kappa} - w\right)^2} V_c^2 - \frac{(2 \times 3EI)}{L_1^3} w - \eta \frac{dw}{dt} = m \frac{d^2 w}{dt^2} \quad (1)$$

where  $\epsilon$  is the permittivity of free space,  $\kappa$  is the relative dielectric constant of the thin dielectric layer above the bottom plate,  $E$  is the modulus of elasticity,  $I$  is the moment of inertia of the cantilever,  $\eta$  is the viscoelasticity constant and  $m$  is the mass of the membrane. The first term on the left describes the total downward electrostatic force acting on the membrane. The second term describes the upward force exerted by the cantilevers and is valid when the vertical deflection is less than 30% of the cantilever length [6]. The third term captures the effects of energy loss through cyclical plastic deformation, molecular friction and the viscosity of air in the system via a viscoelasticity coefficient. This damping effect will reduce the membrane oscillation especially during switching off.